



Structural and microvascular retinal changes in keratoconus: an OCT and OCT angiography study

Ozlem Ozkan ¹, Canan Asli Utine ^{2,3}, Raffaele Piscopo ⁴ and Luca D' Andrea ⁵

¹ Department of Ophthalmology, Dr. Behcet Uz Pediatric Diseases and Surgery Training and Research Hospital, Izmir, Turkiye

² Dokuz Eylul University Faculty of Medicine, Department of Ophthalmology, Izmir, Turkiye

³ Izmir Biomedicine and Genome Center, Izmir, Turkiye

⁴ Department of Neurosciences, Reproductive Sciences and Dentistry, University of Naples, Federico II, Napoli, Italy

⁵ Department of Life Science, Health, and Health Professions, Link Campus University, Rome, Italy

ABSTRACT

Background: Keratoconus is increasingly recognized as a condition that may affect not only corneal structure but also posterior segment parameters. This study aimed to evaluate alterations in central macular, choroidal, and peripapillary retinal nerve fiber layer thicknesses, as well as peripapillary vessel densities (VDs), in eyes with keratoconus using optical coherence tomography (OCT) and OCT angiography (OCTA).

Methods: This cross-sectional study included eyes with keratoconus and healthy control eyes. Participants underwent Scheimpflug corneal tomography (Pentacam HR) to assess central corneal thickness (CCT) and keratometry; spectral-domain OCT (SD-OCT) for central macular thickness (CMT), choroidal thickness, and peripapillary retinal nerve fiber layer thickness (RNFLT) measurements; and swept-source OCT angiography (SS-OCTA) to quantify peripapillary VD centrally and across four quadrants at the superficial and deep capillary plexuses (pSCP, pDCP), the peripapillary choriocapillaris (pCC), and the global radial peripapillary capillary plexus (nRPCP).

Results: Eighty-six eyes with keratoconus and 86 age-, sex-, axial-length-, and laterality-matched healthy controls (all $P > 0.05$) were analyzed. The keratoconus group showed significantly higher spherical equivalent, higher keratometry parameters, higher astigmatism, and lower CCT, along with worse best-corrected distance visual acuity (all $P < 0.001$). Mean choroidal thickness was significantly greater in eyes with keratoconus ($P < 0.001$), whereas CMT, global RNFLT, and most quadrant RNFLT measures were comparable (all $P > 0.05$), except for a thinner inferonasal RNFLT ($P < 0.05$). Central VD in the pSCP, pDCP, pCC, and global nRPCP were significantly reduced (all $P < 0.05$). Eyes with keratoconus additionally demonstrated a non-significant (all $P > 0.05$) but characteristic pattern of regional VD alterations across peripapillary sectors.

Conclusions: Keratoconus was associated with significant microvascular and structural alterations extending beyond the cornea, including reduced VDs in central peripapillary plexuses, localized thinning of inferonasal RNFLT, and increased choroidal thickness. These findings support a broader pathophysiologic framework in which keratoconus involves not only anterior corneal remodeling but also measurable changes in blood supply within the macular and lamina cribrosa regions. The characteristic, though nonsignificant, regional VD patterns further underscore potential sectoral vulnerability. Future longitudinal and multimodal imaging studies are warranted to clarify the temporal evolution, clinical relevance, and prognostic utility of these microvascular changes in keratoconus.

KEYWORDS

choriocapillaris, choroids, retina, macula lutea, optical coherence tomography, optical coherence tomography angiography, optic nerves, peripapillary retinal nerve fiber layer, retinal nerve fiber layer, keratoconus

Correspondences: Canan Asli Utine, Dokuz Eylul University Faculty of Medicine, Department of Ophthalmology, Izmir, Turkiye. Email: cananutine@gmail.com. ORCID iD: <https://orcid.org/0000-0002-4131-2532>.

How to cite this article: Ozkan O, Utine CA, Piscopo R, Andrea LD. Structural and microvascular retinal changes in keratoconus: an OCT and OCT angiography study. Med Hypothesis Discov Innov Optom. 2025 Fall; 6(3): 104-111. DOI: <https://doi.org/10.51329/mehdiptometry229>.

Received: 18 October 2025; Accepted: 18 November 2025



Copyright © Author(s). This is an open-access article distributed under the terms of the Creative Commons Attribution-NonCommercial 4.0 International License (<https://creativecommons.org/licenses/by-nc/4.0/>) which permits copy and redistribute the material just in noncommercial usages, provided the original work is properly cited.



INTRODUCTION

Keratoconus is a progressive ectatic disorder of the cornea characterized by irregularity and reduced density of stromal collagen lamellae. Despite extensive investigation, its pathogenesis is not yet fully understood [1]. Associations between keratoconus and systemic connective tissue disorders, especially mitral valve prolapse, Marfan syndrome, and Ehlers–Danlos syndrome, are well documented [2]. Given that the extracellular collagen matrix is a structural component of the cornea, sclera, lamina cribrosa, and retinal vasculature, it is plausible for keratoconus to coexist with or contribute to posterior segment changes [3–9]. Studies have reported increased choroidal thickness [10–15] and reduced lamina cribrosa thickness [16] in eyes with keratoconus.

Emerging evidence indicates that keratoconus is not solely a corneal disorder but may also encompass structural and vascular alterations within the posterior segment [10–15]. Nevertheless, the extent and clinical relevance of these changes remain insufficiently characterized. The development of optical coherence tomography (OCT) and OCT angiography (OCTA) has enabled non-invasive, high-resolution assessment of macular and peripapillary microvasculature, offering new insights into keratoconus-related changes of the lamina cribrosa and retinal vasculature [8, 9, 17, 18].

We aimed to investigate posterior segment involvement in this ectatic corneal disease based on the hypothesis that keratoconus may represent a collagen-related disorder with vascular implications. In contrast to previous studies that evaluated microvasculature [9, 17, 18], we evaluated a comprehensive set of parameters, including peripapillary superficial and deep capillary plexuses as well as the choriocapillaris. Retinal nerve fiber layer thickness (RNFLT), macular and choroidal thickness, and vascular density (VD) metrics were analyzed and compared with those of healthy control eyes.

METHODS

This cross-sectional, two-center observational study included eyes with keratoconus and healthy control eyes evaluated at the Cornea Units of the Departments of Ophthalmology at Dokuz Eylul University Hospital (Turkiye) and the University of Naples Federico II (Italy) between June 2022 and February 2025. The study protocol was approved by the Dokuz Eylul University Ethics Committee (2023/22-23). All procedures adhered to the ethical principles of the Declaration of Helsinki and applicable local regulations. Informed consent was obtained from all participants; for individuals aged 16 to 18 years, consent was additionally secured from a parent or legal guardian in accordance with ethical requirements.

Keratoconus was diagnosed according to the Global Consensus on Keratoconus and Ectatic Diseases [19], requiring the presence of abnormal posterior corneal elevation, an abnormal pattern of corneal thickness distribution, and non-inflammatory corneal thinning. Characteristic anterior corneal steepening was also considered supportive of the diagnosis. Exclusion criteria comprised age <15 years, a history of ocular surgery unrelated to keratoconus, spherical equivalent of refractive error exceeding ± 20 diopters (D), systemic hypertension, migraine or other vasculopathies, ocular hypertension, corneal opacities involving the visual axis, and OCT or OCTA images of insufficient quality due to artifacts. Healthy individuals in the control group were selected to match the keratoconus cohort in age, sex, axial length, and laterality. Additional exclusion criteria for the control group included history of ocular surgery, systemic vascular disorders (e.g., diabetes, hypertension), or other conditions known to affect the retinal or optic nerve microvasculature.

The clinical history of all participants, including demographic characteristics and the presence of systemic or additional ocular disorders, was documented. Each individual underwent a comprehensive ophthalmic evaluation comprising best-corrected distance visual acuity (BCDVA) assessment using a Snellen chart (Nidek Co., Ltd., Gamagori, Aichi, Japan) and intraocular pressure (IOP) measurement with Goldmann applanation tonometry (AT-900; Haag-Streit AG) under slit-lamp biomicroscopy (Haag-Streit BM 900; Haag-Streit AG, Bern, Switzerland). A detailed evaluation of the anterior and posterior segments was performed using slit-lamp biomicroscopy.

All participants underwent Scheimpflug corneal tomography (Pentacam, Oculus GmbH, Wetzlar, Germany), macular and optic nerve head imaging with spectral-domain OCT (SD-OCT; Spectralis®, Heidelberg Engineering, Heidelberg, Germany) incorporating the 3D wide glaucoma module for peripapillary radial RNFLT assessment, and swept-source OCT angiography (SS-OCTA; DRI OCT Triton Plus®, Topcon Corporation, Tokyo, Japan) using 6×6 mm scans for optic nerve head microvascular measurements.

The Belin/Ambrosio Enhanced Ectasia Display (BAD) of the Scheimpflug imaging-based Pentacam system was used to stage keratoconus, incorporating maximum keratometry, anterior and posterior elevation parameters, and tomographic central corneal thickness (CCT). CCT, flat keratometry (K1), steep keratometry (K2), and astigmatism values obtained from corneal tomography were compared between the study groups (Figure 1).

Central macular thickness (CMT), choroidal thickness, and peripapillary RNFLT were measured using SD-OCT imaging and compared between the study groups. CMT and choroidal thickness were automatically quantified from radial macular scans (Figures 2A, B). Global and sectoral (superior, nasal, inferior, and temporal) peripapillary RNFLT values were automatically derived from the glaucoma scan protocol (Figure 2C).

Peripapillary vessel densities (VD) of the superficial capillary plexus (pSCP), deep capillary plexus (pDCP), peripapillary choriocapillaris (pCC), and global radial peripapillary capillary plexus (nRPCP) were quantified from 6×6 -mm SS-OCTA scans and compared between groups. Vascular plexus segmentation was performed using automated algorithms with manual

refinement when necessary. To assess localized microvascular defects, VD was computed for each layer (superficial, deep, and choriocapillaris) within the superior, nasal, inferior, and temporal peripapillary sectors, in addition to calculating the global nRPCP metric (Figure 3).

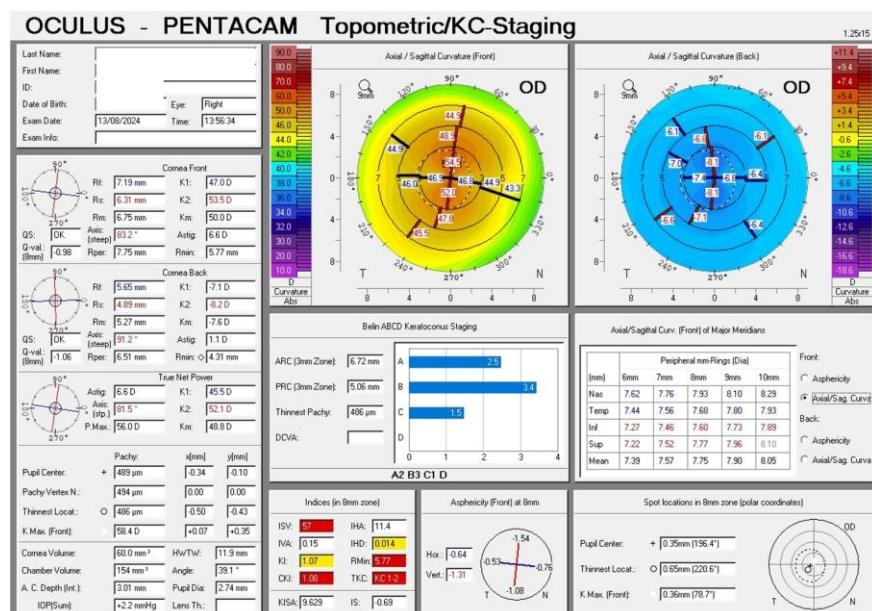


Figure 1. Pentacam Belin/Ambrosio Enhanced Ectasia Display (BAD) and topometric maps obtained using the Scheimpflug imaging-based Pentacam system (Oculus GmbH, Wetzlar, Germany). Central corneal thickness, flat keratometry (K1), and steep keratometry (K2) were extracted as key tomographic indices. Anterior and posterior curvature maps, together with the Belin ABCD staging parameters, were used to characterize corneal geometry and to compare tomographic features between keratoconus and control eyes.

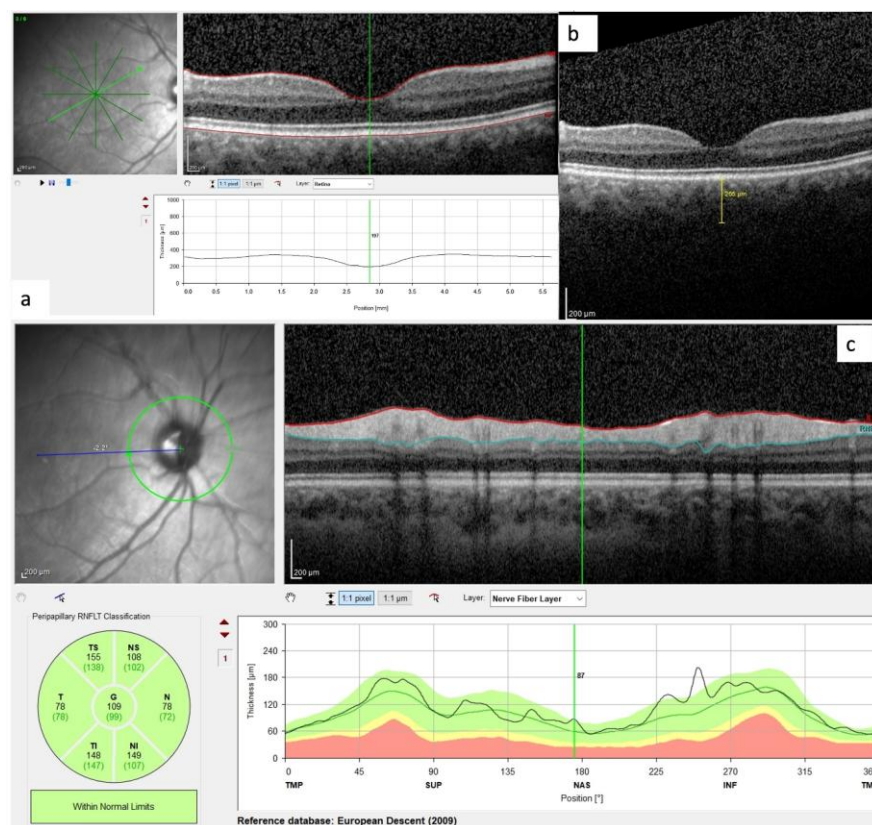


Figure 2. (A, B) Radial spectral-domain optical coherence tomography (SD-OCT; Spectralis®, Heidelberg Engineering, Heidelberg, Germany) macular scans showing automated measurements of central macular thickness (CMT) and subfoveal choroidal thickness (CT). (C) SD-OCT peripapillary glaucoma scan showing automated segmentation and quantification of global and sectoral retinal nerve fiber layer thickness (RNFLT) across the superior, nasal, inferior, and temporal quadrants.

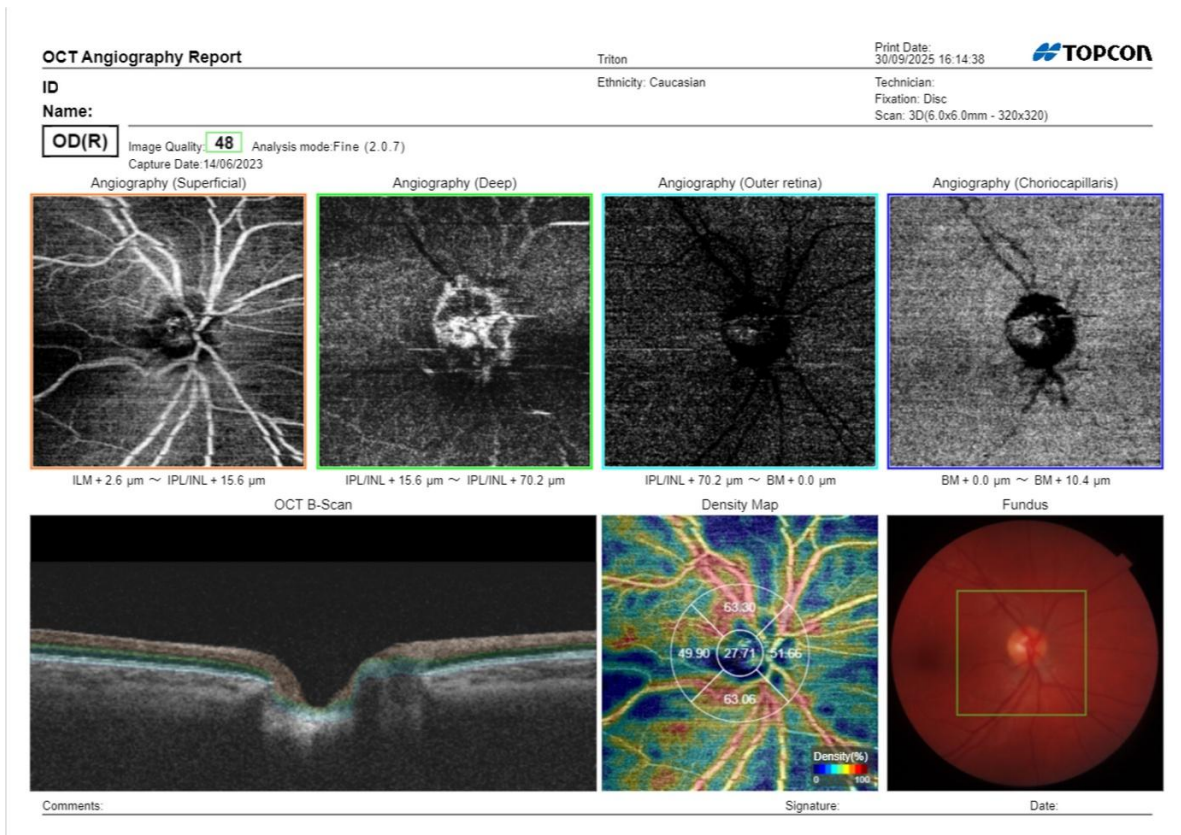


Figure 3. Peripapillary optical coherence tomography angiography (OCTA) report obtained using swept-source OCT (SS-OCTA; DRI OCT Triton Plus®, Topcon Corporation, Tokyo, Japan), showing automated layer-specific segmentation of the superficial, deep, outer retina, and choriocapillaris slabs. The panel includes en face angiograms for each vascular layer, the corresponding structural B-scan with segmentation boundaries, a peripapillary vessel density map, and the color fundus image indicating the 6 × 6-mm scan area.

Statistical analyses were conducted using SPSS Statistics for Windows, version 25 (IBM Corp., Armonk, NY, USA). Data normality was assessed using the Shapiro–Wilk test. Quantitative variables were reported as mean (standard deviation [SD]), and categorical variables as frequencies (percentages). Between-group comparisons of continuous variables were performed using the independent samples *t*-test, while sex distribution was compared using the chi-square test. A two-tailed *P*-value < 0.05 was considered statistically significant.

RESULTS

A total of 86 eyes from 86 patients with keratoconus and 86 age-, sex-, axial-length-, and laterality-matched eyes from 86 healthy controls were included. Eyes with keratoconus were classified as stage 1 (*n* = 28, 32.55%), stage 2 (*n* = 28, 32.55%), stage 3 (*n* = 24, 27.90%), and stage 4 (*n* = 6, 6.99%). Among the 86 keratoconus eyes, 38 (44.18%) had previously undergone corneal cross-linking. The mean spherical equivalent was significantly higher and the mean BCDVA significantly worse in the keratoconus group (both *P* < 0.001). Mean CCT was significantly lower, whereas mean keratometry values and astigmatism measurements were higher in eyes with keratoconus (all *P* < 0.001). Comprehensive demographic and clinical characteristics of study participants are summarized in Table 1.

Table 2 presents a comparison of all OCT- and OCTA-derived parameters between eyes with keratoconus and healthy controls. Mean choroidal thickness was significantly greater in eyes with keratoconus (*P* < 0.001). In contrast, CMT, global peripapillary RNFLT, and quadrant-specific peripapillary RNFLT values were generally comparable between groups (all *P* > 0.05), with the exception of the inferonasal RNFLT, which was significantly reduced in eyes with keratoconus (Table 2).

Regarding mean VD_s, the central VD of the pSCP, pDCP, and pCC, as well as the global nRCP VD, were significantly reduced in eyes with keratoconus compared with healthy eyes (all *P* < 0.05) (Table 2). Although not statistically significantly, eyes with keratoconus demonstrated a characteristic pattern of regional VD alterations, showing lower mean temporal VD in the pSCP, pDCP, and pCC, and lower inferior VD in the pDCP. Conversely, higher mean nasal or superior VD values were observed in the pSCP, pDCP, and pCC, and higher inferior VD in the pSCP and pCC (all *P* > 0.05) (Table 2).

Table 1. Demographic and clinical data of study participants

Variable	Keratoconus (n = 86)	Healthy controls (n = 86)	P-value
Age (y), Mean \pm SD (Range)	27.44 \pm 8.37 (16 to 44)	27.44 \pm 8.37 (16 to 44)	< 0.99
Sex (Male / Female), n (%)	55 (63.95) / 31 (36.05)	55 (63.95) / 31 (36.05)	< 0.99 ¹
Laterality (OD / OS), n (%)	43 (50) / 43 (50)	43 (50) / 43 (50)	< 0.99
BCDVA (decimal), Mean \pm SD (Range)	0.65 \pm 0.27 (0.05 to 1.0)	0.99 \pm 0.05 (0.8 to 1.0)	< 0.001
SE (D), Mean \pm SD (Range)	-3.83 \pm 3.73 (-18.00 to 1.50)	-0.68 \pm 0.44 (-0.25 to 1.75)	< 0.001
IOP (mmHg), Mean \pm SD (Range)	13.85 \pm 1.53 (12 to 17)	14.49 \pm 1.44 (10 to 18)	0.618
AL (mm), Mean \pm SD (Range)	23.46 \pm 0.95 (21.70 to 25.34)	23.46 \pm 0.95 (21.70 to 25.34)	< 0.99
Keratoconus stage, n (%)			
Stage 1	28 (32.55)	-	-
Stage 2	28 (32.55)		
Stage 3	24 (27.90)		
Stage 4	6 (6.99)		
CCT(μ m), Mean \pm SD (Range)	470.63 \pm 49.55 (375 to 553)	540.79 \pm 23.79 (497 to 614)	< 0.001
K1 (D), Mean \pm SD (Range)	46.32 \pm 4.75 (40.20 to 64.00)	42.53 \pm 1.11 (41.30 to 44.50)	< 0.001
K2(D), Mean \pm SD (Range)	48.90 \pm 7.63 (41.30 to 67.40)	43.42 \pm 1.19 (42.10 to 44.70)	< 0.001
Astigmatism(D), Mean \pm SD (Range)	3.05 \pm 1.74 (0.80 to 6.50)	0.89 \pm 0.31 (0.40 to 1.40)	< 0.001
History of CXL, n (%)	38 (44.18%)	None	-

Abbreviations: n, number; y, years; SD, standard deviation; %, percentage; OD, right eye; OS, left eye; BCDVA, best-corrected distance visual acuity; SE, spherical equivalent; D, diopters; IOP, intraocular pressure; mmHg, millimeter of mercury; AL, axial length; mm, millimeters; CCT, central corneal thickness; μ m, micrometers; K1, flat keratometry value; K2, steep keratometry value; CXL, corneal-cross-linking. Note: P-values < 0.05 are shown in bold; Spherical equivalent was calculated by adding the spherical component of the refraction to half of the cylindrical component.

Table 2. Optical coherence tomography (OCT) and OCT angiography (OCTA) data in eyes with keratoconus and healthy control eyes

Variable	Keratoconus (n = 86)	Healthy controls (n = 86)	P-value
CMT (μ m), Mean \pm SD (Range)	227.36 \pm 26.97 (135 to 261)	226.38 \pm 21.45 (210 to 288)	0.192
CT (μ m), Mean \pm SD (Range)	260.26 \pm 76.72 (148 to 343)	198.41 \pm 28.43 (167 to 249)	< 0.001
RNFLT Global (μ m), Mean \pm SD	101.01 \pm 10.50	99.45 \pm 8.98	0.980
RNFLT Temporal (μ m), Mean \pm SD	75.45 \pm 11.51	73.13 \pm 12.84	0.179
RNFLT Temporal Inferior (TI), Mean \pm SD	140.89 \pm 17.98	142.96 \pm 18.49	0.605
RNFLT Temporal Superior (TS), Mean \pm SD	133.07 \pm 17.98	135.33 \pm 15.61	0.121
RNFLT Nasal (μ m), Mean \pm SD	79.58 \pm 21.97	74.75 \pm 17.34	0.540
RNFLT Nasal Inferior (NI), Mean \pm SD	112.14 \pm 19.29	113.02 \pm 23.54	0.010
RNFLT Nasal Superior (NS), Mean \pm SD	106.31 \pm 19.82	108.36 \pm 17.50	0.712
pSCP VD, Mean \pm SD			
Nasal	52.64 \pm 4.60	51.37 \pm 4.38	0.639
Temporal	48.98 \pm 4.45	52.06 \pm 3.87	0.194
Superior	60.64 \pm 3.77	59.17 \pm 3.15	0.333
Inferior	60.94 \pm 3.60	60.68 \pm 4.03	0.697
Central	41.84 \pm 8.66	46.86 \pm 5.31	< 0.001
pDCP VD, Mean \pm SD			
Nasal	53.69 \pm 4.38	51.17 \pm 4.30	0.940
Temporal	48.20 \pm 4.44	51.93 \pm 3.90	0.220
Superior	59.60 \pm 3.82	58.65 \pm 3.18	0.077
Inferior	60.25 \pm 3.72	60.40 \pm 3.68	0.656
Central	44.42 \pm 6.68	50.54 \pm 4.10	< 0.001
pCC VD, Mean \pm SD			
Nasal	53.72 \pm 4.73	51.19 \pm 4.09	0.277
Temporal	49.20 \pm 4.74	52.08 \pm 4.04	0.249
Superior	60.90 \pm 3.64	59.32 \pm 3.22	0.270
Inferior	61.57 \pm 3.18	60.76 \pm 4.04	0.270
Central	43.05 \pm 7.64	46.49 \pm 5.33	0.009
Global nRPCP VD, Mean \pm SD	46.56 \pm 5.93	47.38 \pm 4.16	0.014

Abbreviations: n, number; CMT, central macular thickness; μ m, micrometer; SD, standard deviation; CT, central choroidal thickness; RNFLT, retinal nerve fiber layer thickness; VD, vessel density; pSCP, peripapillary superficial capillary plexus; pDCP, peripapillary deep capillary plexus; pCC, peripapillary choriocapillaris; nRPCP, nerve radial peripapillary capillary plexus. Note: P-values < 0.05 are shown in bold.

DISCUSSION

In this study, eyes with keratoconus exhibited thinner corneas, higher astigmatism, steeper keratometry values, and worse BCDVA compared with healthy eyes. Despite largely preserved macular thickness and peripapillary RNFLT, the inferonasal RNFLT was significantly reduced, suggesting localized neuroretinal vulnerability. Choroidal thickness was markedly increased in keratoconus, aligning with proposed choroidal involvement in ectatic disease. Notably, central VD across the pSCP, pDCP, pCC, and global nRPCP was significantly reduced, accompanied by a distinct but nonsignificant pattern of regional microvascular alterations. These findings highlight multi-layer structural and microvascular changes in keratoconus that extend beyond anterior corneal pathology.

Although the pathogenesis of keratoconus remains incompletely understood [1], the condition is recognized as a progressive ectatic disorder marked by stromal collagen lamellar irregularity and thinning [1]. Emerging evidence demonstrating comparable collagen composition in the cornea, sclera, and lamina cribrosa [3–6] has prompted the hypothesis that keratoconus may exert effects across multiple ocular connective tissues due to shared biomechanical properties [7–9]. Consistent with this broader framework, prior studies have reported increased macular choroidal thickness [10–15] and lamina cribrosa thinning [16] in keratoconus. In our study, keratoconus was associated with distinct microvascular and structural alterations extending beyond the cornea, including reduced VDs in central peripapillary plexuses, focal thinning of the inferonasal RNFL, and increased choroidal thickness; this suggests that keratoconus encompasses more extensive ocular involvement than previously appreciated, with measurable perturbations in posterior segment perfusion and tissue architecture in addition to anterior corneal deformation.

Structural and vascular changes in the macula and optic nerve head in eyes with keratoconus have just begun to be investigated. The RNFLT, macular and choroidal thickness, and decreased VD compared to the control group confirm the hypothesis that there are macular and peripapillary changes in keratoconus [8, 9, 17]. In our study, eyes with keratoconus had a significantly thicker central choroidal thickness, comparable with previous studies [10–15]. On the other hand, in our study the central macular and peripapillary RNFLT in all quadrants were comparable between groups, with the exception of inferonasal RNFLT, which was significantly reduced in eyes with keratoconus.

The macular and peripapillary tissue and microvasculature system are evaluated non-invasively with OCTA [8, 18]. Unlike other studies [8, 9, 17] in which the global capillary plexus of the macular superficial, deep, and choriocapillaris layers and the peripapillary microvasculature were evaluated, ours assessed peripapillary microvasculature in separate layers of superficial and deep capillary plexus, choriocapillaris, as well as the global peripapillary capillary plexus.

In eyes with keratoconus, the mean numerical VD values for pSCP, pDCP, and pCC VD, were lower in the temporal regions and higher in the nasal and superior regions than healthy controls, albeit not statistically significantly. Moreover, the central pSCP, pDCP, and pCC VD, as well as, global nRPCP VD, were significantly thinner in eyes with keratoconus compared to healthy controls. Decreased flow in the nRPCP might predict this collagen tissue-rich region being affected in keratoconus. Although this finding is similar to a study showing that early-stage keratoconus can be characterized by a subtle thinning of the peripapillary RNFL and posterior bending of the lamina cribrosa along with vascular disruption [8], it does not fully comply with our RNFLT finding. Another study showed less blood flow in the central peripapillary region in eyes with keratoconus [9]. This supports the low VD in the central part of each layer, which we found to be significant in eyes with keratoconus. Moreover, unlike the study that showed thinning of the RNFL in the temporal quadrant [20], which along with the nRPCP VD is known to be the most common place to distinguish between healthy and glaucomatous eyes, we did not detect thinning in the RNFL compared to the control group. Still, we found that the peripapillary blood flow decreased in every layer in the temporal quadrant, yet without reaching statistical significance.

Recent studies comparing the thickness of the sclera and lamina cribrosa have shown that keratoconus is not just a corneal disease [16, 21]. The results of this study, similar to the studies investigating and comparing vascular flows with OCT and OCTA [8, 17, 18], concur that keratoconus may be a collagen tissue disease affecting the microvasculature and the blood supply of the posterior segment. This finding highlights the need for future studies assessing whether keratoconus confers an increased risk of age-related macular degeneration or ischemic disorders of the retina and optic nerve.

Our findings reinforce the growing evidence that keratoconus is not limited to anterior corneal pathology but also involves posterior segment alterations detectable on OCT and OCTA. Consistent with prior reports, we observed significantly increased choroidal thickness and reduced peripapillary vascular metrics in keratoconus, while macular and RNFL structure remained largely preserved except for localized inferonasal thinning of RNFLT. These results align with and extend the structural-microvascular paradigm proposed in earlier imaging-based studies [10–13]. Our observation of increased mean choroidal thickness corroborates the robust and reproducible choroidal thickening reported by Akkaya et al. [10], Bilgin et al. [11], Gutierrez-Bonet et al. [12], and Pinheiro-Costa et al. [13]. Subfoveal choroidal thickness in these studies [10, 12, 13] consistently exceeded control values—with increases of approximately 53 μm in Pinheiro-Costa et al. [13] and more than 100 μm in Gutierrez-Bonet et al. [12]. Similarly to Akkaya et al. [10], we found a thicker choroid despite heterogeneity in disease severity. In addition, our finding of significantly reduced inferonasal RNFLT parallels the inferonasal peripapillary choroid thinning pattern described by Akkaya et al. [10], suggesting concordant regional susceptibility within the posterior pole.

Bilgin et al. [11] reported no significant correlation between choroidal thickness and corneal thinning, whereas Pinheiro-Costa et al. [13] found that subfoveal choroidal thickness correlated significantly with spherical equivalent and proposed that choroidal thickening may reflect a global choroidal or inflammatory mechanism rather than a biomechanical response to corneal changes [13]. We did not perform correlation or association analyses for these parameters in the current study, and such relationships should be examined in future research.

Our results also align with SS-OCT findings by Gutierrez-Bonet et al. [12], who reported consistently increased macular choroidal thickness in keratoconus, with values tending to normalize after age 45 [12]. Although our cohort was younger, our data support their interpretation that keratoconus involves broader choroidal remodeling across the macular region. The absence of significant choroidal thickness differences between mild and severe keratoconus in Akkaya et al.'s study [10] and between progressive and non-progressive cases in Pinheiro-Costa et al.'s study [14] further supports the notion that choroidal thickness does not track disease stage and therefore may have limited prognostic utility. However, we did not perform stage-based subgroup analyses in the present study, preventing direct comparison of our findings with theirs.

Beyond choroidal alterations, the present study provides new insights into peripapillary microvascular impairment in keratoconus. Dogan et al. [17] reported reduced macular SCP and DCP VDs, as well as diminished radial peripapillary capillary VD [17]. Our findings extend this work by localizing microvascular reductions specifically to central peripapillary VDs across the pSCP, pDCP, pCC, and global nRPCP. We also observed non-significant regional tendencies—temporal and inferior attenuation with relative nasal or superior preservation—that have not been systematically described in prior OCTA studies. Our observation of inferonasal RNFL thinning complements Dogan et al.'s report [17] of reduced radial peripapillary perfusion and suggests early sectoral vulnerability of the peripapillary-lamina cribrosa complex in keratoconus. These comparative findings indicate that keratoconus is associated with reproducible choroidal thickening and emerging peripapillary microvascular compromise. The combined structural OCT and peripapillary OCTA data support a broader posterior pole phenotype, underscoring the need for longitudinal multimodal studies to determine whether these changes precede, parallel, or follow corneal ectatic progression.

Our study provides novel evidence into the presence of significant peripapillary vascular alterations, increased central choroidal thickness, and disrupted blood flow in the macular and lamina cribrosa regions in eyes with keratoconus. These findings support the hypothesis that keratoconus extends beyond the cornea to involve posterior segment structures, possibly as part of a broader collagen-related disorder. There are limitations to this study. First, only a small keratoconus cohort was included due to the study's exploratory nature and the need to exclude many eyes due to poor image quality. Future studies with a prospective design should confirm this association in larger cohorts and investigate associations with progression of keratoconus. Second, an automated algorithm measured RNFLT and OCT parameters, while OCTA measurements were performed manually. Considering the possibility of incorrect evaluation of lamina cribrosa measurements, they were not included in the parameters. In that respect, this needs to be improved by using automatic segmentation in imaging and obtaining the lamina cribrosa parameters in future studies. Future studies should likewise investigate the longitudinal implications of these vascular changes and their potential role in keratoconus progression monitoring.

CONCLUSIONS

This study demonstrates that keratoconus is associated with distinct posterior segment alterations extending beyond its well-recognized corneal manifestations. Eyes with keratoconus exhibited significantly increased choroidal thickness and reduced central peripapillary VDs across the superficial, deep, and choriocapillaris plexuses, together with decreased global nRPCP metrics. Although macular and overall peripapillary RNFLT remained largely preserved, localized inferonasal RNFL thinning suggests early neuroretinal susceptibility. The characteristic though nonsignificant, sectoral vascular patterns further indicate region-specific microvascular imbalance. Our findings support a broader pathophysiologic model in which keratoconus involves measurable perturbations of posterior segment perfusion and tissue architecture in addition to anterior corneal deformation. Future longitudinal multimodal imaging studies are warranted to clarify the temporal dynamics of these changes, assess their prognostic relevance, and determine whether posterior segment biomarkers may contribute to risk stratification and disease monitoring in keratoconus.

ETHICAL DECLARATIONS

Ethical approval: The study protocol was approved by the Dokuz Eylul University Ethics Committee (2023/22-23). All procedures adhered to the ethical principles of the Declaration of Helsinki and applicable local regulations. Informed consent was obtained from all participants; for individuals aged 16 to 18 years, consent was additionally secured from a parent or legal guardian in accordance with ethical requirements.

Conflict of interests: None.

FUNDING

None.

ACKNOWLEDGMENTS

This study was submitted as a poster at The International Society of Cornea, Stem Cells and Ocular Surface SICSSO Congress on June 27-29th, 2024.

REFERENCES

1. Morishige N, Shin-Gyou-Uchi R, Azumi H, Ohta H, Morita Y, Yamada N, Kimura K, Takahara A, Sonoda KH. Quantitative analysis of collagen lamellae in the normal and keratoconic human cornea by second harmonic generation imaging microscopy. *Invest Ophthalmol Vis Sci*. 2014 Nov 25;55(12):8377-85. doi: 10.1167/iops.14-15348. PMID: 25425311.
2. Kalkan Akcay E, Akcay M, Uysal BS, Kosekahya P, Aslan AN, Caglayan M, Koseoglu C, Yulek F, Cagil N. Impaired corneal biomechanical properties and the prevalence of keratoconus in mitral valve prolapse. *J Ophthalmol*. 2014;2014:402193. doi: 10.1155/2014/402193. Epub 2014 Apr 17. PMID: 24864193; PMCID: PMC4016888.
3. Ponsioen TL, van Luyn MJ, van der Worp RJ, van Meurs JC, Hooymans JM, Los LI. Collagen distribution in the human vitreoretinal interface. *Invest Ophthalmol Vis Sci*. 2008 Sep;49(9):4089-95. doi: 10.1167/iops.07-1456. Epub 2008 Apr 30. PMID: 18450587.
4. McBrien NA, Gentle A. Role of the sclera in the development and pathological complications of myopia. *Prog Retin Eye Res*. 2003 May;22(3):307-38. doi: 10.1016/s1350-9462(02)00063-0. PMID: 12852489.
5. Chaerkady R, Shao H, Scott SG, Pandey A, Jun AS, Chakravarti S. The keratoconus corneal proteome: loss of epithelial integrity and stromal degeneration. *J Proteomics*. 2013 Jul 11;87:122-31. doi: 10.1016/j.jprot.2013.05.023. Epub 2013 May 29. PMID: 23727491; PMCID: PMC3721369.
6. Ihanamäki T, Pelliniemi LJ, Vuorio E. Collagens and collagen-related matrix components in the human and mouse eye. *Prog Retin Eye Res*. 2004 Jul;23(4):403-34. doi: 10.1016/j.preteyeres.2004.04.002. PMID: 15219875.
7. Hashemi H, Heirani M, Ambrósio R Jr, Hafezi F, Naroo SA, Khorrami-Nejad M. The link between Keratoconus and posterior segment parameters: An updated, comprehensive review. *Ocul Surf*. 2022 Jan;23:116-122. doi: 10.1016/j.jtos.2021.12.004. Epub 2021 Dec 8. PMID: 34890805.
8. Pierro L, Bianco L, Bertuzzi F, Arrigo A, Saladino A, Distefano A, Berni A, Knutsson KA, Rama P, Bandello F. New Findings in Early-Stage Keratoconus: Lamina Cribrosa Curvature, Retinal Nerve Fiber Layer Thickness, and Vascular Perfusion. *Am J Ophthalmol*. 2023 Feb;246:122-129. doi: 10.1016/j.ajo.2022.10.012. Epub 2022 Oct 30. PMID: 36323392.
9. Wylegala A, Szkodny D, Fiolka R, Wylegala E. Assessment of the Retinal Vessels in Keratoconus: An OCT Angiography Study. *J Clin Med*. 2022 May 24;11(11):2960. doi: 10.3390/jcm11112960. PMID: 35683349; PMCID: PMC9181444.
10. Akkaya S. Macular and Peripapillary Choroidal Thickness in Patients With Keratoconus. *Ophthalmic Surg Lasers Imaging Retina*. 2018 Sep 1;49(9):664-673. doi: 10.3928/23258160-20180831-03. PMID: 30222800.
11. Bilgin B, Karadag AS. Choroidal thickness in keratoconus. *Int Ophthalmol*. 2020 Jan;40(1):135-140. doi: 10.1007/s10792-019-01156-y. Epub 2019 Aug 20. PMID: 31432355.
12. Gutierrez-Bonet R, Ruiz-Medrano J, Peña-García P, Catanese M, Sadeghi Y, Hashemi K, Gabison E, Ruiz-Moreno JM. Macular Choroidal Thickening in Keratoconus Patients: Swept-Source Optical Coherence Tomography Study. *Transl Vis Sci Technol*. 2018 Jun 7;7(3):15. doi: 10.1167/tvst.7.3.15. PMID: 29888113; PMCID: PMC5991807.
13. Pinheiro-Costa J, Viana Pinto J, Perestrelo S, Beato JN, Torrão L, Brandão E, Carneiro Â, Madeira MD, Falcão-Reis F. Increased Choroidal Thickness in Keratoconus Patients: Perspectives in the Disease Pathophysiology. *J Ophthalmol*. 2019 Dec 3;2019:2453931. doi: 10.1155/2019/2453931. PMID: 31871781; PMCID: PMC6913161.
14. Pinheiro-Costa J, Correia PJ, Pinto JV, Alves H, Torrão L, Moreira R, Falcão M, Carneiro Â, Madeira MD, Falcão-Reis F. Increased choroidal thickness is not a disease progression marker in keratoconus. *Sci Rep*. 2020 Nov 17;10(1):19938. doi: 10.1038/s41598-020-77122-x. PMID: 33203915; PMCID: PMC7673983.
15. Gutierrez-Bonet R, Ruiz-Medrano J, Biarnés M, Rasheed MA, Vupparaboina KK, Chhablani J, Ruiz-Moreno JM. Analysis of Choroidal Vascularity Index in Keratoconus Patients Using Swept-Source Optical Coherence Tomography-Based Binarization Techniques. *J Ophthalmol*. 2020 Jan 8;2020:1682463. doi: 10.1155/2020/1682463. PMID: 32025344; PMCID: PMC6984744.
16. Akkaya S, Küçük B. Lamina Cribrosa Thickness in Patients With Keratoconus. *Cornea*. 2017 Dec;36(12):1509-1513. doi: 10.1097/ICO.0000000000001379. PMID: 28922330.
17. Dogan B, Bozdoğan YC, Gedik B, Erol MK, Bulut M, Duman F. Optic disc and retinal vessel densities assessment by optical coherence tomography angiography in patients with keratoconus. *Photodiagnosis Photodyn Ther*. 2023 Mar;41:103218. doi: 10.1016/j.pdpdt.2022.103218. Epub 2022 Nov 30. PMID: 36462703.
18. Vahedi H, Abdollahi M, Moshfeghinia R, Emami S, Sobhi N, Sorkhabi R, Jafarizadeh A. Retinal thickness and vascular density changes in Keratoconus: A systematic review and meta-analysis. *Heliyon*. 2025 Jan 18;11(2):e42099. doi: 10.1016/j.heliyon.2025.e42099. PMID: 39925350; PMCID: PMC11804566.
19. Gomes JA, Tan D, Rapuano CJ, Belin MW, Ambrósio R Jr, Guell JL, Malecaze F, Nishida K, Sangwan VS; Group of Panelists for the Global Delphi Panel of Keratoconus and Ectatic Diseases. Global consensus on keratoconus and ectatic diseases. *Cornea*. 2015 Apr;34(4):359-69. doi: 10.1097/ICO.0000000000000408. PMID: 25738235.
20. Bayat K, Pooyan P, Feizi S, Ahmadi H, Hafezi F, Pourhoseingholi MA, Fekri S, Sarraf D. Structural alterations in the retina and choroid of keratoconus patients detected by optical coherence tomography: A systematic review and meta-analysis. *Surv Ophthalmol*. 2025 Nov 4;S0039-6257(25)00195-X. doi: 10.1016/j.survophthal.2025.11.004. Epub ahead of print. PMID: 41197878.
21. Yıldız MB, Bolaç R. Is Keratoconus More Than Just a Corneal Disease? *Cornea*. 2024 Mar 1;43(3):360-364. doi: 10.1097/ICO.0000000000003366. Epub 2023 Aug 22. PMID: 37607306.